

# Modelling of Specimen Fracture

## *Final Report*

Christopher Bayley  
DRDC Atlantic

Prepared by:

Martec Ltd.  
1888 Brunswick Street, Suite 400  
Halifax, NS. B3J 3J8

CSA: W7707-13-5632/001

The scientific or technical validity of this Contract Report is entirely the responsibility of the Contractor and the contents do not necessarily have the approval or endorsement of the Department of National Defence of Canada.

Contract Report  
DRDC-RDDC-2013-C5  
September 2013

## **IMPORTANT INFORMATIVE STATEMENTS**

The information contained herein is proprietary to Her Majesty and is provided to the recipient on the understanding that it will be used for information and evaluation purposes only. Any commercial use including use for manufacture is prohibited.

© Her Majesty the Queen in Right of Canada (Department of National Defence), 2013

© Sa Majesté la Reine en droit du Canada (Ministère de la Défense nationale), 2013

**Modelling of Specimen Fracture  
Final Report**

**Martec Technical Report #TR-13-47**

**September 2013**

**Prepared for:**

**Christopher Bayley  
DRDC Atlantic Dockyard Laboratory Pacific  
CFB Esquimalt, Building 199  
PO Box 17000, Station Forces  
Victoria, British Columbia  
Canada  
V9A-7N2**

**Martec Limited** tel. 902.425.5101  
1888 Brunswick Street, Suite 400 fax. 902.421.1923  
Halifax, Nova Scotia B3J 3J8 Canada email. martec-info@lr.org  
[www.martec.com](http://www.martec.com)



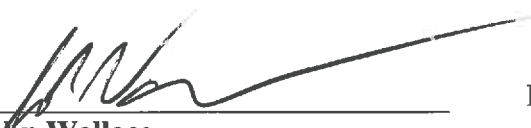
**SIGNATURE PAGE**

**MODELLING SPECIMEN FRACTURE – PROGRESS REPORT**

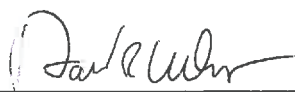
**Technical Report # TR-13-47  
23 September 2013**

Prepared by:   
**Rick Link  
Senior Research Engineer**

Date: Sept 23, 2013

Reviewed by:   
**John Wallace  
Senior Research Engineer**

Date: Sep 23 2013

Approved by:   
**Dave Whitehouse  
Manager, Research and Product Development**

Date: Sept 23, 2013

## EXECUTIVE SUMMARY

This report is a summary of the work that has been performed on the implementation of global fracture parameters into a finite element (FE) post-processing computer code. The work is a continuation of a previous study involving the implementation of a micromechanical fracture model into the LS-DYNA user-defined subroutines.

Two fracture parameters were identified and implemented into the post-processor: the strain energy release rate,  $J$ , and the Weibull stress,  $\sigma_w$ . The calculation of these parameters involved parsing the output data of the selected FE code, LS-DYNA, including element stresses, strain energies, and nodal coordinates and kinematic variables for an arbitrary number of dump times in a specified geometric window. The calculation of  $J$  involves the automatic determination of J-integral contours, which was coded into the post-processor.

The calculation routines were validated using a linear elastic problem for the  $J$ -integral calculator, and Beremin's [2] data for the Weibull stresses. The calculated results were in good agreement with published values. Future work includes the continuing testing and improvement of the post-processor.

## TABLE OF CONTENTS

<b>1.0</b>	<b>INTRODUCTION .....</b>	<b>1</b>
<b>2.0</b>	<b>J INTEGRAL CALCULATION .....</b>	<b>3</b>
2.1	PRELIMINARIES .....	3
2.2	FINITE ELEMENT FORMULATION .....	5
2.3	ELEMENT JACOBIAN .....	5
2.4	SPATIAL DERIVATIVES.....	6
2.5	1 <sup>ST</sup> PIOLA-KIRCHOFF STRESS TENSOR.....	7
2.6	DEFORMATION GRADIENT TENSOR .....	7
2.7	FINITE ELEMENT DOMAIN FOR J-INTEGRAL CALCULATION .....	8
2.7.1	<i>Determination of Crack Coordinate System.....</i>	<i>8</i>
2.7.2	<i>Determination of Weighting Function, q.....</i>	<i>9</i>
2.8	DETERMINATION OF J-INTEGRAL CONTOURS .....	9
2.9	J-INTEGRAL CALCULATION .....	9
2.10	J-INTEGRAL CALCULATION EXAMPLE .....	10
<b>3.0</b>	<b>WEIBULL STRESSES AND BEREMIN MODEL CALCULATION .....</b>	<b>13</b>
3.1	PROBABILITY DISTRIBUTION CURVE .....	13
3.2	PROBABILITY FUNCTION CURVE FIT.....	14
3.3	CURVE FITTING PROCEDURE .....	14
3.4	CURVE FITTING EXAMPLE – BEREMIN DATA.....	15
<b>4.0</b>	<b>SUMMARY AND CONCLUSIONS .....</b>	<b>20</b>
<b>5.0</b>	<b>REFERENCES .....</b>	<b>21</b>

### APPENDIX A: HEXAHEDRAL SHAPE FUNCTIONS AND DERIVATIVES

### APPENDIX B: LS-DYNA CRACK POST-PROCESSOR

## LIST OF FIGURES

FIGURE 2.1: J INTEGRAL DOMAIN VOLUME AND CRACK REFERENCE FRAME (FROM [4]) .....	3
FIGURE 2.2: WEIGHTING FUNCTION, Q (FROM [4]) .....	4
FIGURE 2.3: CRACK REFERENCE FRAME .....	8
FIGURE 3.1: SPECIMEN DIMENSIONS FOR AE0.2 SPECIMENS (OBTAINED FROM [2]) .....	15
FIGURE 3.2: SPECIMEN FE MODELS .....	15
FIGURE 3.3: YIELD AND FLOW STRESS DEPENDENCE ON TEMPERATURE (FROM [2]).....	16

## LIST OF TABLES

TABLE 2.1: CALCULATED J VALUE FOR CONTOURS .....	12
TABLE 3.1: MATERIAL PROPERTIES FOR BEREMIN FE ANALYSIS.....	17
TABLE 3.2: WEIBULL STRESSES – SORTED LIST.....	17



## 1.0 INTRODUCTION

This report is a continuation of previous work in which a constitutive model for steel was developed that addressed material failure in both the brittle and ductile regimes [1]. For ductile (high temperature) regions, where void nucleation and coalescence governs failure, the Johnson-Cook plasticity model was used in conjunction with Gurson void fraction evolution. For brittle (low temperature) regions, the maximum principal stress was assumed to govern failure; fracture occurred when the maximum principal stress reached a critical cleavage fracture value.

Although a critical cleavage fracture stress is simple in concept, it is not widely used as a practical fracture measure. Investigators have tended to adopt more probabilistic approaches such as the Beremin [2] and Master Curve [3] methods. In these methods, a scalar fracture measure for cracked regions is computed or experimentally determined or both for a number of test specimens. This fracture measure is then ranked and fit to a cumulative distribution curve to determine the probability of failure at a specified scalar fracture measure.

In this project, it is desired to adopt the probabilistic methodology to compute fracture initiation. Two measures of interest include the strain energy release rate,  $J$ , and Weibull stress,  $\sigma_w$ . The original tasks were as follows:

- 1) **Task 1: Elastic-Plastic Fracture Mechanics Parameter and Internal Strain Energy Density** – a methodology to compute  $J$  for three-dimensional finite element (FE) meshes will be adopted and implemented as a FE post-processor. This will also involve calculation of the internal strain energy density,  $W$ , in the FE constitutive model developed in the previous work. The J-integral method will be validated using classical test problems defined by the Scientific Authority and Martec.
- 2) **Task 2: Size Dependent Cleavage Fracture Modelling** – the calculation of  $\sigma_w$  for specified Weibull parameters will be added to the FE post-processor.
- 3) **Task 3: Application of the Size Dependent DBT Model** - the Beremin model will be used to fit Weibull parameters to the drop tower tests analysed in [1]. The J-integral method may be used to rank the experiments for the Beremin model.

After the completion of Tasks 1 and 2, the scope of Task 3 was changed slightly because of the following reasons:

- 1) It was unclear how to apply the  $J$ -integral and Beremin fracture criteria to dynamic fracture. Both methods are more suitable for determining the onset of brittle fracture in static analysis.
- 2) Extensive time and effort had been spent in developing a crack post-processor for LS-DYNA, and there were not sufficient funds to develop a methodology for dynamic fracture.

Task 3 was rewritten to include the testing of the Beremin model using Beremin's original data, using specimen failure loads to rank the experiments.

In order to compute these global fracture parameters, a crack post-processor for LS-DYNA has been written in C++. The post-processor reads the LS-DYNA d3plot file for the desired time window, then computes either Weibull stresses or J-integrals for specific times.

Section 2 describes the methodology used for the 3-D J-integral calculation along with a validation calculation. Section 3 contains the Beremin model methodology and testing. Section 4 summarizes the work, and identifies areas of future study.

## 2.0 J INTEGRAL CALCULATION

The calculation of the local mechanical energy release rate,  $J$ , follows the procedure outlined in [4]. The methodology utilizes a domain integral approach, where an average value of  $J$  is computed for the 3-D domain. The calculation is performed using the crack post-processor described in Appendix B.

### 2.1 PRELIMINARIES

Figure 2.1 shows the crack domain. The crack coordinate system is oriented with  $X_2$  normal to the crack plane,  $X_3$  tangent to the crack. The direction  $X_1$  is the direction of crack extension. The calculation volume of interest is denoted as  $V$ , and is enclosed by areas  $A_1 - A_5$ . The crack dimension is denoted as  $s$ ;  $V$  extends from point  $a$  to point  $c$  ( $s_a$  to  $s_c$ ). An average value of  $J$  is computed at point  $b$ .

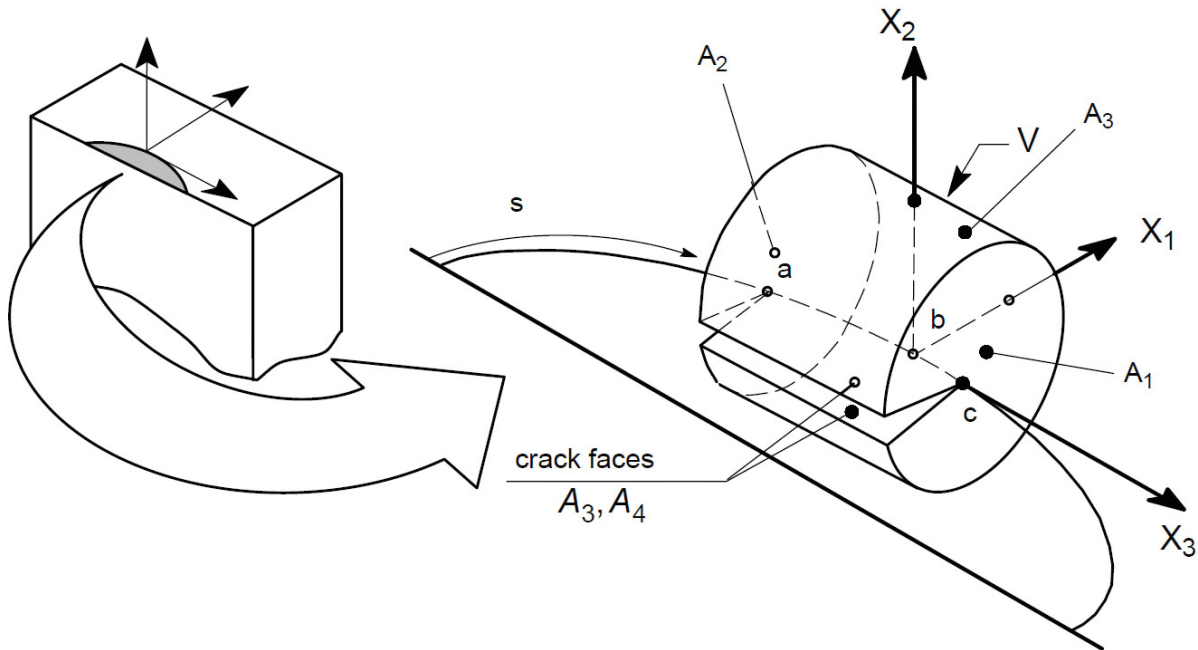


**Figure 2.1: J Integral Domain Volume and Crack Reference Frame (from [4])**

In the calculation, the following is assumed:

- 1) Body forces are neglected (other than inertial forces).
- 2) Thermal strains are neglected.
- 3) High speed crack propagation is not included.
- 4) Tensor notation is used.

The domain integral approach utilizes the virtual crack extension principle [4]. In this method, the contributing terms to the mechanical release rate over the domain from  $a$  to  $c$ ,  $\bar{J}_{a-c}$ , are multiplied by an arbitrary weighting function,  $q$ , as shown in Figure 2.2.

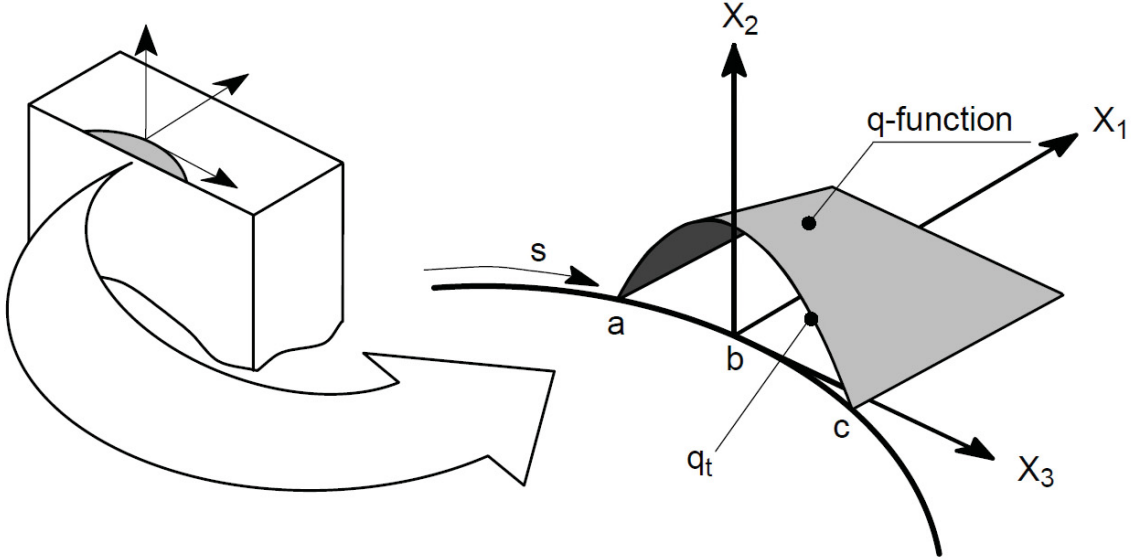


Figure 2.2: Weighting function,  $q$  (from [4])

The average value at  $b$ ,  $J$ , is then calculated by using the mean value theorem.

$$J = \frac{\bar{J}_{a-c}}{\int_{s_c}^{s_a} q(s) ds} \quad [2.1]$$

Utilizing assumptions 1-4,  $\bar{J}_{a-c}$ , can be expressed as

$$\bar{J}_{a-c} = \int_{s_a}^{s_c} J(s)q(s) ds = \int_{V_0} \left( q_{,j} P_{ji} u_{i,1} - W q_{,1} - \frac{1}{2} \rho \dot{u}_i \dot{u}_i q_{,1} + \rho \ddot{u}_i u_{i,1} q \right) dV_0 \quad [2.2]$$

where

$P$  = 1<sup>st</sup> Piola-Kirchoff stress tensor

$u, \dot{u}, \ddot{u}$  = displacement, velocity, and acceleration, respectively

$\rho$  = material density

$W$  = strain energy density

and the commas in the subscripts imply differentiation. Since the 1<sup>st</sup> Piola-Kirchoff stresses are used here, the differentiation is with respect to the original coordinates,  $X$ , rather than the current coordinates,  $x$ . The strain energy density,  $W$ , is computed as

$$W = \int_{\varepsilon} \sigma_{ij} d\varepsilon_{ij} \quad [2.3]$$

where  $\sigma$  and  $\varepsilon$  are the true stress and true strain, respectively.

## 2.2 FINITE ELEMENT FORMULATION

If the domain is discretized into a number of finite elements,  $n_e$ , Equation 2.2 becomes

$$\bar{J}_{a-c} = \sum_{i=1}^{n_e} \int_{V_0} \left( \langle q_{,j} \rangle [P]^T \{u_{,1}\} - W q_{,1} - \frac{1}{2} \rho \langle \dot{u} \rangle \{ \dot{u} \} q_{,1} + \rho \langle \ddot{u} \rangle \{ u_{,1} \} q \right) dV_{0i} \quad [2.4]$$

LS-DYNA uses one-point integration for their hexahedral elements. Using this integration rule in conjunction with the standard isoparametric formulation, Equation 2.4 is now written as

$$\bar{J}_{a-c} = \sum_{i=1}^{n_e} 2|J|_0 \left( \langle q_{,j} \rangle [P]^T \{u_{,1}\} - W q_{,1} - \frac{1}{2} \rho \langle \dot{u} \rangle \{ \dot{u} \} q_{,1} + \rho \langle \ddot{u} \rangle \{ u_{,1} \} q \right)_{0i} \quad [2.5]$$

where  $J$  is the element Jacobian matrix. The element coordinates, kinematic variables and weighting function are expressed in terms of trilinear shape functions,  $N$

$$X_i = \langle N(r, s, t) \rangle \{ \bar{X}_i \} \quad [2.6]$$

$$x_i = \langle N \rangle \{ \bar{x}_i \} \quad [2.7]$$

$$u_i = \langle N \rangle \{ \bar{u}_i \}$$

$$\dot{u}_i = \langle N \rangle \{ \dot{\bar{u}}_i \} \quad [2.8]$$

$$\ddot{u}_i = \langle N \rangle \{ \ddot{\bar{u}}_i \}$$

$$q = \langle N \rangle \{ \bar{q} \} \quad [2.9]$$

where  $r, s, t$  are isoparametric coordinates, and the overbar denotes nodal quantities. Appendix A contains the hexahedral element shape functions.

## 2.3 ELEMENT JACOBIAN

The element Jacobian is evaluated using

$$[J] = \begin{bmatrix} \frac{\partial X_1}{\partial r} & \frac{\partial X_2}{\partial r} & \frac{\partial X_3}{\partial r} \\ \frac{\partial X_1}{\partial s} & \frac{\partial X_2}{\partial s} & \frac{\partial X_3}{\partial s} \\ \frac{\partial X_1}{\partial t} & \frac{\partial X_2}{\partial t} & \frac{\partial X_3}{\partial t} \end{bmatrix} \quad [2.10]$$

Substituting Equation 2.6 into 2.10 yields

$$[J] = \begin{bmatrix} \frac{\partial \langle N \rangle}{\partial r} \{X_1\} & \frac{\partial \langle N \rangle}{\partial r} \{X_2\} & \frac{\partial \langle N \rangle}{\partial r} \{X_3\} \\ \frac{\partial \langle N \rangle}{\partial s} \{X_1\} & \frac{\partial \langle N \rangle}{\partial s} \{X_2\} & \frac{\partial \langle N \rangle}{\partial s} \{X_3\} \\ \frac{\partial \langle N \rangle}{\partial t} \{X_1\} & \frac{\partial \langle N \rangle}{\partial t} \{X_2\} & \frac{\partial \langle N \rangle}{\partial t} \{X_3\} \end{bmatrix} \quad [2.11]$$

## 2.4 SPATIAL DERIVATIVES

Spatial derivatives are computed using Equation 2.12

$$\begin{Bmatrix} \frac{\partial}{\partial X_1} \\ \frac{\partial}{\partial X_2} \\ \frac{\partial}{\partial X_3} \end{Bmatrix} = [J]^{-1} \begin{Bmatrix} \frac{\partial}{\partial r} \\ \frac{\partial}{\partial s} \\ \frac{\partial}{\partial t} \end{Bmatrix} \quad [2.12]$$

For the weighting function,  $q$ , Equation 2.12 yields

$$\begin{Bmatrix} \frac{\partial q}{\partial X_1} \\ \frac{\partial q}{\partial X_2} \\ \frac{\partial q}{\partial X_3} \end{Bmatrix} = [J]^{-1} \begin{Bmatrix} \frac{\partial \langle N \rangle}{\partial r} \{ \bar{q} \} \\ \frac{\partial \langle N \rangle}{\partial s} \{ \bar{q} \} \\ \frac{\partial \langle N \rangle}{\partial t} \{ \bar{q} \} \end{Bmatrix} \quad [2.13]$$

Displacement gradients are computed similarly to Equation 2.13. The shape function derivatives are contained in Appendix A.

## 2.5 1<sup>ST</sup> PIOLA-KIRCHOFF STRESS TENSOR

The 1<sup>st</sup> Piola-Kirchoff stress tensor is written as

$$[P] = |F| [\sigma] [F]^{-T} \quad [2.14]$$

where

$[F]$  = deformation gradient tensor

$[\sigma]$  = Cauchy stress tensor

Taking the transpose of both sides of Equation 2.14, and noting that the Cauchy stress tensor is symmetric

$$[P]^T = |F| [F]^{-1} [\sigma] \quad [2.15]$$

Equation 2.15 is used in Equation 2.5.

## 2.6 DEFORMATION GRADIENT TENSOR

The deformation gradient tensor is written as

$$[F] = \begin{bmatrix} \frac{\partial x_1}{\partial X_1} & \frac{\partial x_1}{\partial X_2} & \frac{\partial x_1}{\partial X_3} \\ \frac{\partial x_2}{\partial X_1} & \frac{\partial x_2}{\partial X_2} & \frac{\partial x_2}{\partial X_3} \\ \frac{\partial x_3}{\partial X_1} & \frac{\partial x_3}{\partial X_2} & \frac{\partial x_3}{\partial X_3} \end{bmatrix} \quad [2.16]$$

Substituting the transpose of Equation 2.13 into Equation 2.16

$$[F] = \begin{bmatrix} \left\langle \frac{\partial \langle N \rangle}{\partial r} \{ \bar{x}_1 \} \right\rangle & \left\langle \frac{\partial \langle N \rangle}{\partial s} \{ \bar{x}_1 \} \right\rangle & \left\langle \frac{\partial \langle N \rangle}{\partial t} \{ \bar{x}_1 \} \right\rangle [J]^{-T} \\ \left\langle \frac{\partial \langle N \rangle}{\partial r} \{ \bar{x}_2 \} \right\rangle & \left\langle \frac{\partial \langle N \rangle}{\partial s} \{ \bar{x}_2 \} \right\rangle & \left\langle \frac{\partial \langle N \rangle}{\partial t} \{ \bar{x}_2 \} \right\rangle [J]^{-T} \\ \left\langle \frac{\partial \langle N \rangle}{\partial r} \{ \bar{x}_3 \} \right\rangle & \left\langle \frac{\partial \langle N \rangle}{\partial s} \{ \bar{x}_3 \} \right\rangle & \left\langle \frac{\partial \langle N \rangle}{\partial t} \{ \bar{x}_3 \} \right\rangle [J]^{-T} \end{bmatrix} \quad [2.17]$$

## 2.7 FINITE ELEMENT DOMAIN FOR J-INTEGRAL CALCULATION

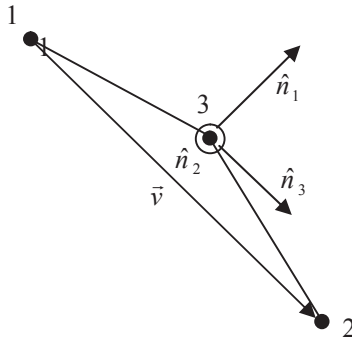
### 2.7.1 Determination of Crack Coordinate System

Figure 2.3 shows the crack edge of interest, defined by three nodes. The normal in the  $X_2$  direction,  $\hat{n}_2$ , is previously defined. The normal parallel to the crack,  $\hat{n}_3$ , is taken as the direction of the normalized component of the vector between node 1 and node 2, perpendicular to  $\hat{n}_2$

$$\hat{n}_3 = \frac{\bar{v} - (\hat{n}_2 \cdot \bar{v})\bar{v}}{\|\bar{v} - (\hat{n}_2 \cdot \bar{v})\bar{v}\|} \quad [2.18]$$

The direction of crack propagation,  $\hat{n}_1$ , is then taken as the cross product between  $\hat{n}_2$  and  $\hat{n}_3$

$$\hat{n}_1 = \hat{n}_2 \times \hat{n}_3 \quad [2.19]$$



**Figure 2.3: Crack Reference Frame**

All tensorial variables must be transformed to the crack reference frame. For vectors such as coordinates, displacements, velocities and accelerations

$$\{X\}_c = [T]\{X\}_g \quad [2.20]$$

and for stresses

$$[\sigma]_c = [T]^T [\sigma]_g [T] \quad [2.21]$$

Where the subscripts “c” and “g” refer to crack and global reference frames, respectively, and  $[T]$  is a transformation matrix, given by

$$[T] = \begin{bmatrix} \langle \hat{n}_1 \rangle \\ \langle \hat{n}_2 \rangle \\ \langle \hat{n}_3 \rangle \end{bmatrix} \quad [2.22]$$



### 2.7.2 Determination of Weighting Function, $q$

The weighting function,  $q$ , can be any arbitrary function within the J-integral domain, and must be zero on the domain boundary. An easy function commonly adopted by investigators is to set  $q = 1.0$  on all nodes in the domain interior, and  $q = 0.0$  on the domain boundary.

## 2.8 DETERMINATION OF J-INTEGRAL CONTOURS

Figure 2.4 shows the mesh of a typical crack problem, arranged in a Cartesian fashion. The J-integral domain is always two elements wide, and is defined by a number of contours as shown by the red arrowed lines in Figure 2.4. Each contour consists of a number of contiguous elements that encircle the previous contours, and include all elements contained in the previous contours.

Given the crack tip nodes, the J-integral contours are determined automatically by finding nodal pairs that are contained in the adjacent elements. For contour 1 in Figure 2.4, the crack tip nodes are used as nodal pairs. For contour 2, the exterior nodes of contour 1 are used as nodal pairs for adjacency checking, and so on.

For this implementation, only regular Cartesian arrangements and full 8 node hexahedrons are admitted. Future development will include degenerated elements and multiple crack tip nodes.

## 2.9 J-INTEGRAL CALCULATION

The calculation method proceeds as follows:

- 1) The crack tip coordinate system is defined by using Section 2.7.1. Coordinates, kinematic variables, and stresses are transformed to the crack tip coordinate system.

For each contour:

- 2) The nodal weighting function,  $q$ , is applied to interior and boundary nodes using Section 2.7.2.
- 3) The J-integral is evaluated using the expressions from Sections 2.2-2.6.

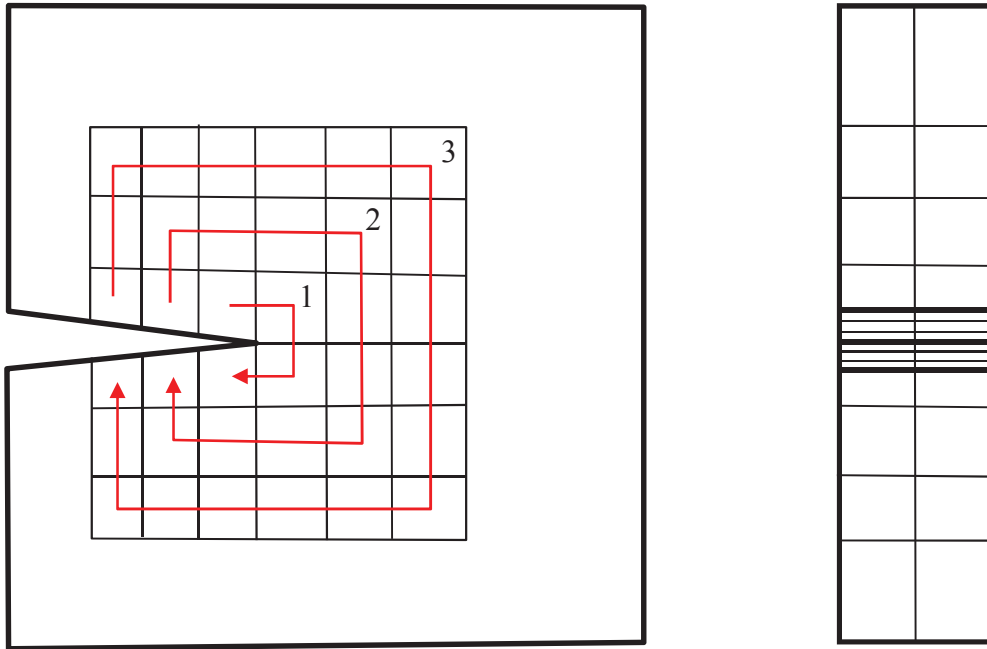


Figure 2.4: Crack Tip Mesh and J-Integral Contours

## 2.10 J-INTEGRAL CALCULATION EXAMPLE

A linear elastic example problem is used for validation; the J-integral is computed using the crack post-processor described in Appendix B. In this example, a central through-thickness crack is introduced in a thin steel plate of finite width and loaded statically perpendicular to the crack. Figure 2.5 shows the crack geometry. The strain energy release rate,  $J$ , is computed as

$$J = \frac{K^2}{E} \quad [2.23]$$

where  $K$  is the crack tip stress intensity factor, calculated as [7]

$$K = \beta \sigma \sqrt{\pi a} \quad [2.24]$$

$$\beta = \sqrt{\sec \frac{\pi a}{W}} \quad [2.25]$$

Figure 2.6 shows the finite element model used. An elastic modulus and Poisson's ratio of 200,000 MPa and 0.3 were used, respectively. The plate thickness and height are 5 and 200 mm, respectively. Ten hexahedral elements were used through the thickness, and  $J$  was calculated at the plate center. An end load of 1.0 MPa was applied.

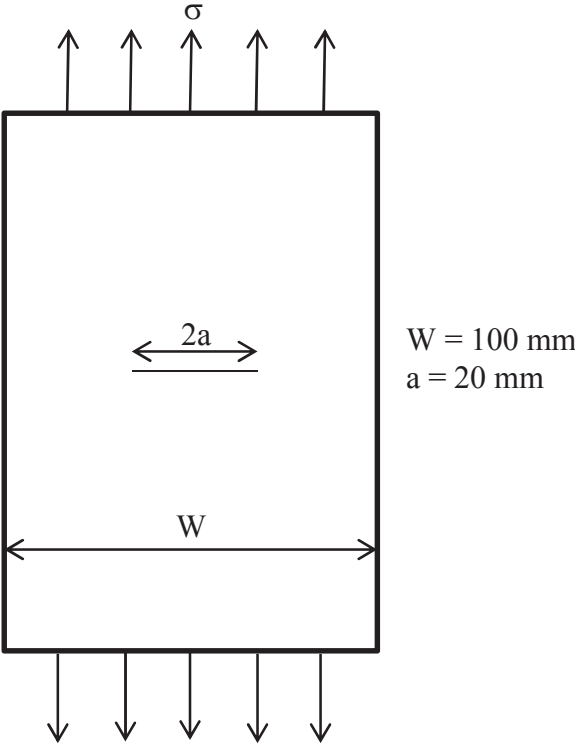


Figure 2.5: Crack Geometry

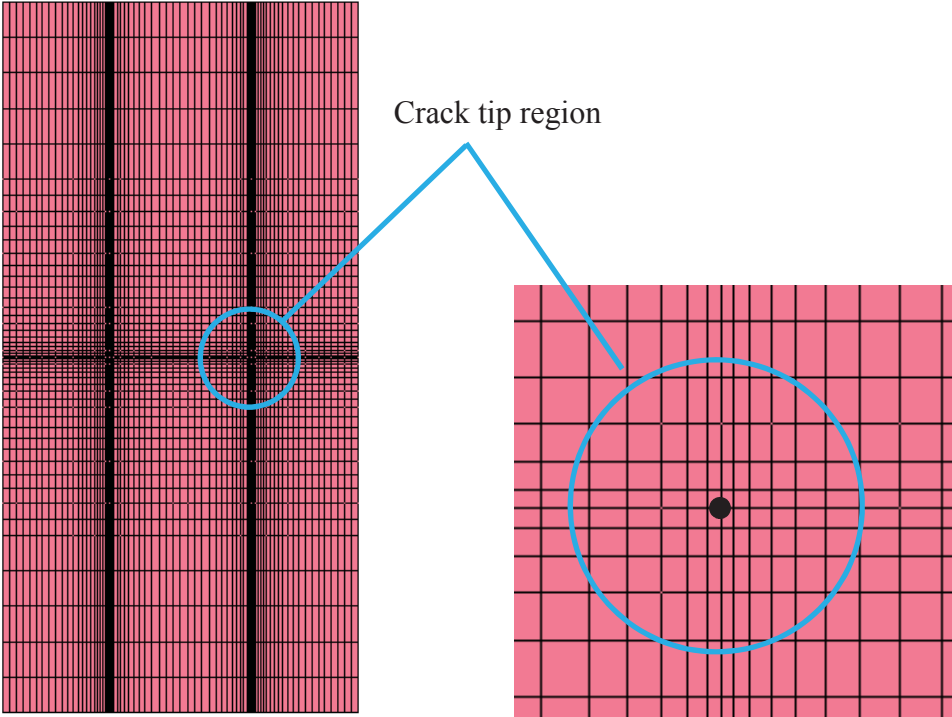


Figure 2.6: Finite Element Model

Table 2.1 shows the computed  $J$  for each of the contours. The average  $J$  for contours 2-10 was  $3.9601 \times 10^{-4}$  MPa-mm, which compares favorably (within 2%) to the theoretical value of  $3.8833 \times 10^{-4}$  MPa-mm.

**Table 2.1: Calculated J Value For Contours**

<b>Contour Number</b>	<b>J (<math>\times 10^{-4}</math> MPa-mm)</b>	<b>% Error</b>
1	3.2622	-15.99
2	3.8793	-0.10
3	3.8693	-0.36
4	4.0390	+4.01
5	3.8997	+0.42
6	4.0312	+3.81
7	3.9761	+2.39
8	3.9877	+2.69
9	3.9679	+2.18
10	3.9908	+2.77
Average 2-9	3.9601	+1.98

### 3.0 WEIBULL STRESSES AND BEREMIN MODEL CALCULATION

The Beremin model [2] is a methodology that combines finite element analysis with experimental results in order to estimate a measure of cleavage fracture stress intensity and its uncertainty. A measure of cleavage fracture initiation (such as displacement at fracture initiation for Charpy V-notch tests) is first selected. Normally, tests are selected in the brittle range (low temperature) in order to exclude all ductile effects. The experimental results are listed in ascending order of the measure, and finite element analyses are performed on each test. The Weibull stress is then computed and fit to a probability distribution curve.

The Weibull stresses are computed using the crack post-processor described in Appendix B.

#### 3.1 PROBABILITY DISTRIBUTION CURVE

The failure probability of any given test can be obtained using a two parameter probability distribution

$$P_f = 1 - \exp\left(-\left(\frac{\sigma_w}{\sigma_u}\right)^m\right) \quad [3.1]$$

where

$P_f$  = failure probability

$\sigma_w$  = Weibull stress

$\sigma_u$  = scaling stress, curve fit parameter 1

$m$  = Weibull exponent, curve fit parameter 2

The Weibull stress is computed using a summation over all the elements in the crack plastic zone,  $n_p$

$$\sigma_w = \left( \sum_{i=1}^{n_p} \sigma_1^i \left( \frac{V_i}{V_0} \right)^m \right)^{1/m} \quad [3.2]$$

where

$\sigma_1$  = maximum principal stress

$V_i$  = element volume

$V_0$  = reference volume, can be taken as 1

### 3.2 PROBABILITY FUNCTION CURVE FIT

The curve fit for Equation 3.1 is not straightforward, because the Weibull stress summation depends on the  $m$  parameter. Usually,  $m$  is assumed, and the scaling parameter,  $\sigma_u$ , is calculated. Equation 3.1 can be rearranged to form

$$\frac{1}{m} \ln \left( \ln \left( \frac{1}{1 - P_f} \right) \right) = \ln(\sigma_w) - \ln(\sigma_u) \quad [3.3]$$

or

$$y = x + b \quad [3.4]$$

where

$$y = \frac{1}{m} \ln \left( \ln \left( \frac{1}{1 - P_f} \right) \right) \quad [3.5]$$

$$y = \ln(\sigma_w) \quad [3.6]$$

$$b = \ln(\sigma_u) \quad [3.7]$$

### 3.3 CURVE FITTING PROCEDURE

Initially, test data is ranked according to a monotonically increasing load parameter that is a direct measure of cleavage fracture initiation. Examples of load parameters that are commonly used are: load, extension, and displacement at fracture initiation. Test data is ranked in ascending order of the load parameter. The curve fitting method then proceeds as follows:

- 1) From the  $N$  specimens, a failure probability is assigned to each specimen,  $j$ , as

$$P = \frac{j - 0.5}{N}, \quad j = 1, N \quad [3.9]$$

- 2) A finite element analysis is performed for each test, and the Weibull stress,  $\sigma_w$ , is computed using Equation 3.2, with a guessed value of  $m$ .
- 3) The parameter  $\sigma_u$  is determined from the x-intercept of curve fitting Equation 3.4.

### 3.4 CURVE FITTING EXAMPLE – BEREMIN DATA

To illustrate the procedure, a curve fit of part of Beremin's [2] data is shown here. A multiple set of two uniaxial specimens were loaded to failure at low temperature (77 K). To check the methodology and the postprocessor, a set of finite element analyses of two specimens, designated AE0.2 Type 2 and AE0.2 Type 3, are processed to obtain the Weibull stresses and curve fits. Figure 3.1 shows the specimen dimensions, and Figure 3.2 the FE models for the Type 2 and 3 geometry. One-quarter symmetry was used for the FE models.

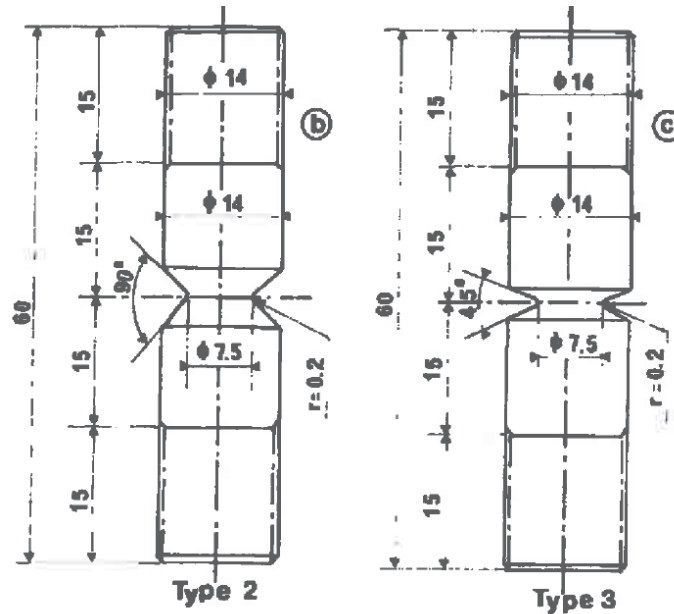


Figure 3.1: Specimen Dimensions for AE0.2 Specimens (obtained from [2])

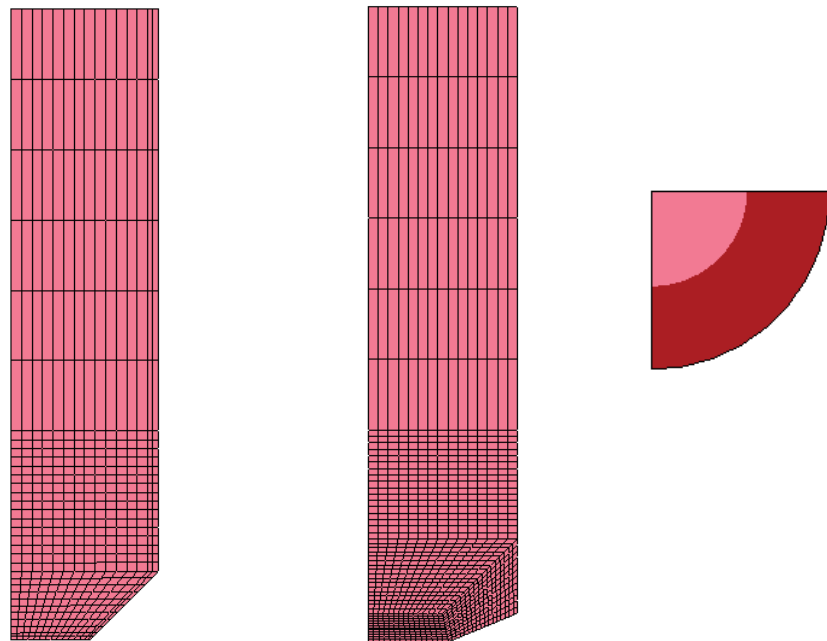


Figure 3.2: Specimen FE Models

Material properties were obtained from Figure 3.3, which shows the temperature dependence of the yield and flow stress. A bilinear stress-strain law was assumed for the FE analyses. The hardening modulus was taken as the difference in flow stress at 10% strain ( $\epsilon$  in Figure 3.3) and the yield stress divided by the strain difference. The data shown in Figure 3.3 is for a different heat of material than the one required; Heat A is required, and Heat B is shown. As a result, the data at 77° K is scaled by the yield strength difference between the two heats (a reduction factor of 0.942). The \*MAT\_PLASTIC\_KINEMATIC material model was used; Table 3.1 shows the material properties used.

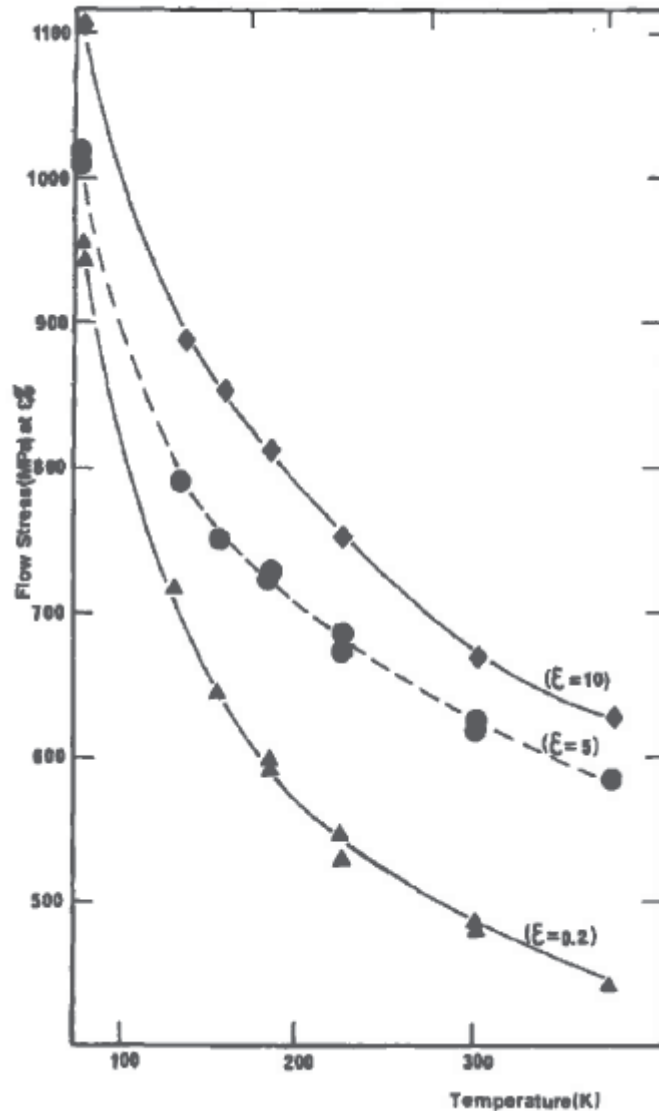


Figure 3.3: Yield and Flow Stress Dependence on Temperature (from [2])



**Table 3.1: Material Properties For Beremin FE Analysis**

Elastic Modulus (MPa)	200,000
Poisson's Ratio	0.3
Yield Stress (MPa)	891.6
Hardening Modulus (MPa)	1449.0

Each FE model is loaded to the failure loads observed in the experiments. At these failure loads, the fracture post-processor is used to compute the Weibull stress assuming an  $m$  exponent of 22.0. Table 3.2 shows the sorted Weibull stresses computed from the FE analyses. The probability of failure is computed using Equation 3.9.

**Table 3.2: Weibull Stresses – Sorted List**

Test Number	Type	Weibull Stress	$P_f$
1	3	1659.6	0.02174
2	3	1718.0	0.06522
3	3	1736.1	0.10870
4	3	1767.7	0.15217
5	3	1979.2	0.19565
6	2	2221.0	0.23913
7	2	2271.5	0.28261
8	2	2392.9	0.32609
9	2	2392.9	0.36957
10	2	2445.7	0.41304
11	2	2478.5	0.45652
12	3	2478.5	0.50000
13	2	2480.9	0.54348
14	2	2521.3	0.58696
15	2	2530.2	0.63043
16	3	2538.8	0.67391
17	2	2539.6	0.71739
18	2	2570.6	0.76087
19	3	2652.4	0.80435
20	3	2667.8	0.84783
21	3	2727.7	0.89130
22	3	2736.9	0.93478
23	3	2745.3	0.97826

Figure 3.4 shows the cumulative plot, along with the curve fit from Equation 3.3. The scaling parameter,  $\sigma_u$ , was determined as 2517.7 MPa. It is evident that the curve fit is less than optimal. There could be several reasons for this:

- 1) Selection of  $m$  – a lower value would rotate the central portion of the curve counter-clockwise and fit the data better at the lower tail. This can be seen by investigation of Beremin's original data in Figure 3.5, which shows essentially the same behavior.

- 2) Finite element model – in the crack region, it was found that relatively few elements resided in the plastic zone at the lower failure loads. A more refined mesh may give more consistent results, since the number of plastic elements would increase. It is difficult to tell what refinement Beremin used, since the mesh data is not available. As well, the material properties used in the Beremin analyses were not explicitly specified. These were estimated based on the available material data.

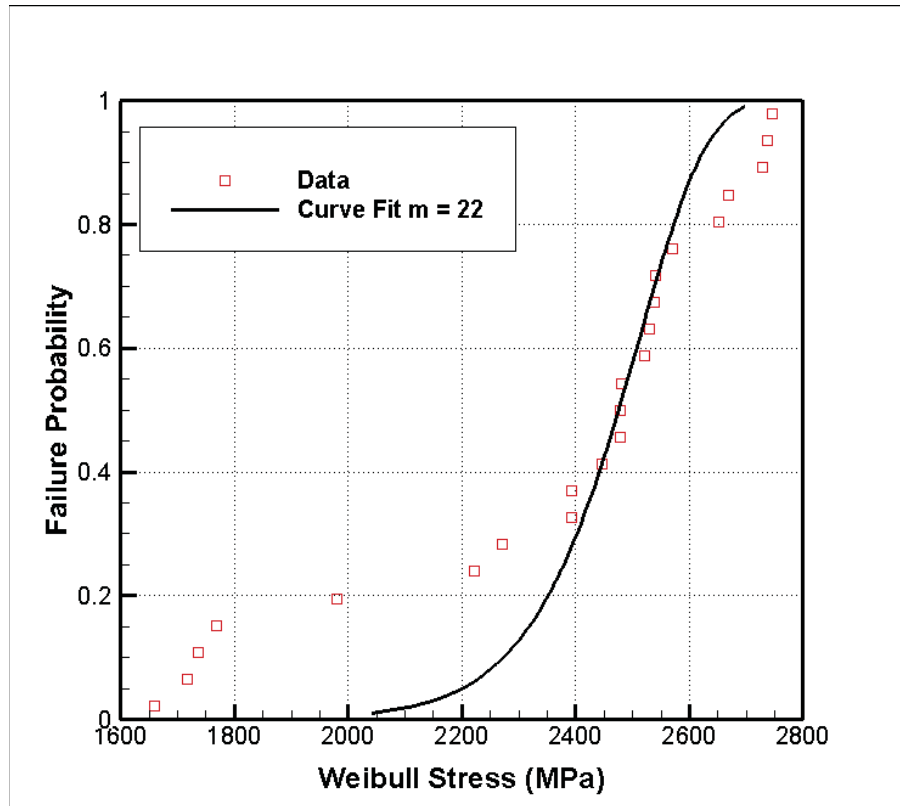


Figure 3.4: Cumulative Failure Probability

Nevertheless, the curve fit with  $m = 22$  yielded a  $\sigma_u$  of 2518 MPa, which compared favorably with the Beremin computed value of 2570 MPa. This indicates that the Weibull stresses computed using the post-processor are correct values.

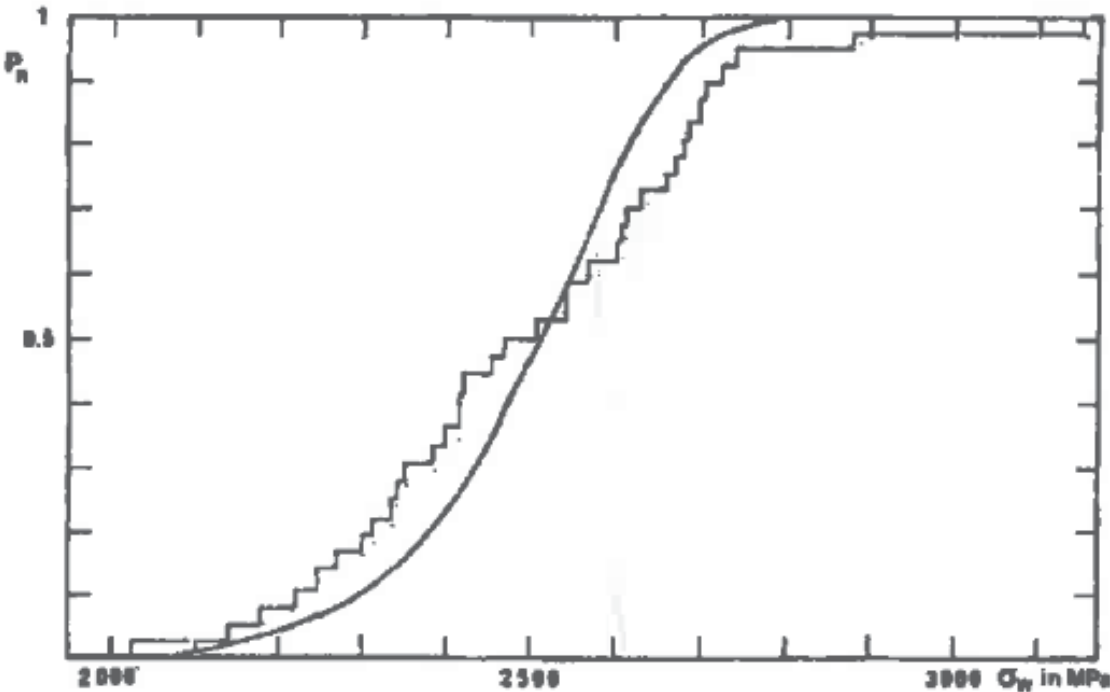


Figure 3.5: Beremin's Original Data

#### 4.0 SUMMARY AND CONCLUSIONS

A post-processor has been written in C++ code to compute J-integrals and Weibull stresses for LS-DYNA 3-dimensional hexahedral elements. The post-processor reads LS-DYNA binary files (d3plot) and computes  $J$  and  $\sigma_w$  for an arbitrary number of contours and solution dump times. For this version, the crack tip is assumed to consist of one nodal point line, and the elements are 8-noded hexahedrons. The computational modules have been validated on selected test problems.

Although great progress has been made on the development of an FE global fracture post-processor, it remains to improve and test the software for larger dynamic problems. The following future work is recommended.

- 1) **Multiple LS-DYNA files** – for large problems, more than one d3plot file is generated. The current software does not support this.
- 2) **Non-hexahedral elements** – incorporation of wedges, tetrahedrons, etc.
- 3) **Tests on nonlinear and dynamic problems** – in particular, the J-integral calculation. This can be performed on the large amount of data collected by DRDC Atlantic for 350WT steel.

## 5.0 REFERENCES

- [1] Link, R.A., B. Yuen, and L. Jiang. 2012. *Development of a Micromechanical Failure Model*. TR-12-24. Martec Limited. Halifax, Nova Scotia.
- [2] Beremin, F.M. 1983. “A Local Criterion for Cleavage Fracture of a Nuclear Pressure Vessel Steel”. *Metallurgical Transactions A*. City. Volume 14A, November, pp. 2277-2287.
- [3] American Society for Testing and Materials. 2006. *ASTM E 1921-05: Standard Test Method for Determination of Reference Temperature,  $T_0$  for Ferritic Steels in the Transition Range*. ASTM. Philadelphia, Pa.
- [4] Healy, B., A. Gullerud, K. Koppenhoefer, A. Roy, S. RoyChowdhury, M. Walters, B. Bichon, K. Cochran, A Carlyle and R. Dodds. 2010. *WARP3D – Release 16.3.1 – 3-D Dynamic Nonlinear Fracture Analysis of Solids Using Parallel Computers*. Structural Research Series No. 607. Department of Civil and Environmental Engineering, University of Illinois at Urbana-Champaign. Urbana, Illinois.
- [5] Livermore Software Technology Corporation. 2011. *LS-DYNA Database Binary Output Files*. LSTC. Livermore, California.
- [6] Bernaur, G., W. Brocks, and W. Schmitt. 1999. “Modifications of the Beremin Model for Cleavage Fracture in the Transition Region of a Ferritic Steel”. *Engineering Fracture Mechanics*. Volume 64, pp. 305-325.
- [7] Broek, D. 1989. *Practical Use of Fracture Mechanics*. Kluwar Academic Publishers. 522 p.

## **APPENDIX A**

### **HEXAHEDRAL SHAPE FUNCTIONS AND DERIVATIVES**

## APPENDIX A: ELEMENT SHAPE FUNCTIONS AND DERIVATIVES

Hexahedral element shape functions can be expressed as

$$N_i = \frac{1}{8}(1 + r_i r)(1 + s_i s)(1 + t_i t), i = 1,8 \quad [A.1]$$

Where  $r, s, t$  are isoparametric coordinates that extend from -1 to +1, and  $i$  is the node number. Figure A.1 shows the isoparametric coordinate and node numbering convention utilized by LS-DYNA. Table A.1 shows the values used for  $r_i, s_i, t_i$  according to node number.

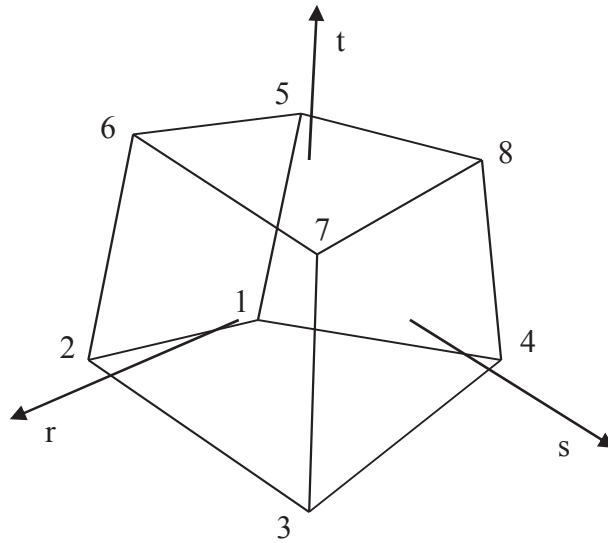


**Figure A.1: Isoparametric Coordinate System**

<b>i</b>	$r_i$	$s_i$	$t_i$
1	-1	-1	-1
2	+1	-1	-1
3	+1	+1	-1
4	-1	+1	-1
5	-1	-1	+1
6	+1	-1	+1
7	+1	+1	+1
8	-1	+1	+1

The shape function derivatives are written as

$$\frac{\partial N_i}{\partial r} = \frac{r_i}{8} (1 + s_i s)(1 + t_i t) \quad [A.2]$$

$$\frac{\partial N_i}{\partial s} = \frac{s_i}{8} (1 + r_i r)(1 + t_i t) \quad [\text{A.3}]$$

$$\frac{\partial N_i}{\partial r} = \frac{t_i}{8} (1 + r_i s)(1 + s_i s) \quad [\text{A.4}]$$



**APPENDIX B**

**LS-DYNA CRACK POST-PROCESSOR**

## APPENDIX B: LS-DYNA CRACK POST-PROCESSOR

This appendix is a description of the crack post-processor (hereafter referred to as CPP). CPP's function is to parse LS-DYNA d3plot files, and calculate either Weibull stresses or J-integrals for a selected time window. The program requires an input file and LS-DYNA d3plot file, and outputs J-integral values and Weibull stresses. The input file is in keyword format similar to that used by LS-DYNA, with an asterisk (\*) preceding any keyword. The keywords can be in any order, and the input file may be commented with the first character being an exclamation point (!). The input is free format.

### B.1: KEYWORD DESCRIPTION

#### \*CALC

Specify the solution type

Variable	Variable Type	Comments
calc_type	Integer	Calculation type = 0 J-integral = 1 Weibull stresses

#### \*CRACK

Define the crack orientation

Variable	Variable Type	Comments
n_crack_nodes	Integer	Number of crack nodes (3 for now)
crack_node[i] i = 1,3	Integer	Crack node numbers
n2[i] i = 1,3	Real	Orientation of crack n <sub>2</sub> normal in Figure 2.1

#### \*J\_CONTOURS

Specify the number of contours for J calculations and properties

Variable	Variable Type	Comments
contour_type	Integer	Contour type – not presently used
n_contours	Integer	Number of contours
part_num	Integer	LS-DYNA part number – not used

### **\*TIMES**

Specify the time range for computation. CPP will perform calculations for d3plot results within this time window

<b>Variable</b>	<b>Variable Type</b>	<b>Comments</b>
start_time	Real	Start time
end_time	Real	End time

### **\*RHO**

Specify the material density

<b>Variable</b>	<b>Variable Type</b>	<b>Comments</b>
rho	Real	Material density

### **\*MAT**

Specify the material type. For a material type of zero (elastic), CPP will compute the elastic strain energy density for use in J-integral calculations. For anything else, CPP will read in the strain energy density from the d3plot file

<b>Variable</b>	<b>Variable Type</b>	<b>Comments</b>
mat_type	Integer	Material type = 0 Linear elastic

### **\*DYNAMICS**

Specify the dynamics type. If zero (static), velocities and accelerations will not be included in the J-integral calculations

<b>Variable</b>	<b>Variable Type</b>	<b>Comments</b>
dyn_type	Integer	Dynamics type = 0 Static = 1 Dynamic

### **\*WEIBULL\_WINDOW**

Specify the geometric window that Weibull stresses will be computed over. CPP will only include elements whose centers lie within the window

Variable	Variable Type	Comments
x_min[i] i = 1,3	Real	Window minimum coordinates
x_max[i] i = 1,3	Real	Window maximum coordinates

### **\*WEIBULL\_WINDOW**

Specify the parameters for Weibull stress calculation.

Variable	Variable Type	Comments
n_Weibull	Integer	Number of Weibull exponents
m_exp[i] i = 1, n_Weibull	Real	Weibull exponents, <i>m</i>
V0	Real	Scaling volume

## **B.2: INPUT FILE COMPOSITION**

Table B.1 shows the applicability of all keywords to the J-integral and Weibull stress computations. Any keyword marked with a checkmark must be included in the selected computation type.

**Table B.1: Keyword Applicability to Selected Analysis Type**

Keyword	J Integral	Weibull Stress
*CALC	✓	✓
*CRACK	✓	
*J CONTOURS	✓	
*TIMES	✓	✓
*RHO	✓	
*MAT	✓	
*DYNAMICS	✓	
*WEIBULL_WINDOW		✓
*WEIBULL_PARAMS		✓